IASSNS-AST 96/31, April 1996

Tests of three-flavor mixing in long-baseline neutrino oscillation experiments

G. L. Fogli
Dipartimento di Fisica dell'Università and Sezione INFN di Bari, I-70126 Bari, Italy

E. Lisi
Institute for Advanced Study, Princeton, New Jersey 08540, U.S.A.
and Dipartimento di Fisica dell'Università and Sezione INFN di Bari, I-70126 Bari, Italy

We compare the effectiveness of various tests of three-flavor mixing in future long-baseline neutrino oscillation experiments. We analyze a representative case of mixing in a simplified three-flavor scheme, whose relevant parameters are one neutrino mass-square difference, m^2, and two mixing angles, ψ and ϕ. We show that an unambiguous determination of ψ and ϕ requires flavor-appearance tests in accelerator experiments, as well as supplementary information from reactor experiments.

PACS number(s): 14.60.Pq, 12.15.Ff, 14.60.Lm

I. INTRODUCTION

The next generation of proposed accelerator neutrino oscillation experiments will be characterized by unprecedented source-detector distances: 730 km for the Fermilab to Soudan experiment (MINOS) [1,2], 250 km for the KEK-PS to SuperKamiokande experiment [3], 68 km for the Brookhaven National Laboratory experiment E889, [4] and 732 km for the CERN to Gran Sasso experiment, with ICARUS [5], RICH [6], or NOE [7] as candidate detectors. Two reactor experiments under construction, Chooz [8] and San Onofre [9], also have a much longer baseline (1 km) than previous experiments of their class.

These long-baseline experiments are sensitive, in the favorable case of large ν mixing, to neutrino square mass differences as low as 10^{-3} eV^2. Moreover, they probe several flavor-oscillation channels. Oscillation signals in two or more independent channels could indicate flavor mixing among three generations (3ν mixing).

In this report, we analyze the effectiveness of long-baseline experiments in detecting 3ν mixing signals. In Sec. II we describe a representative case of mixing in a simple 3ν scheme. (This scheme is extensively discussed in [10,11], to which we refer the reader for further details.) In Secs. III and IV we focus on oscillation searches at ICARUS and MINOS respectively. We also comment briefly upon searches at BNL E889, Superkamiokande, RICH, and NOE. We show that flavor-appearance tests are essential to constrain multiple interpretations of the signals. In Sec. V we show how reactor experiments may eliminate an ambiguity in the determination of the mixing angles. We summarize our work in Sec. VI.

II. THREE-FLAVOR MIXING: A TEST CASE

In a three-generation approach, the ν states with definite flavor ($\nu_\alpha = \nu_e, \nu_\mu, \nu_\tau$) are a superposition of ν states with definite mass ($\nu_i = \nu_1, \nu_2, \nu_3$): $\nu_\alpha = U_{\alpha i}\nu_i$, U being a unitary matrix. We assume [10] that the two independent neutrino square mass differences, $\delta m^2 = m_2^2 - m_1^2$ and $m^2 = m_3^2 - m_1^2$, are widely separated:

$$\delta m^2 \lesssim 10^{-4}\ \text{eV}^2,\ m^2 \gtrsim 10^{-3}\ \text{eV}^2 \ \longrightarrow\ \delta m^2 \ll m^2\ . \quad (1)$$

Accelerator and reactor neutrino oscillations are then simply described in terms of (m^2, U_{e3}, $U_{\mu 3}$, $U_{\tau 3}$) or, equivalently, in terms of (m^2, ψ, ϕ), along with the parameterization ($s_\phi = \sin\phi$, etc.):

$$U_{e3}^2 = s_\phi^2, \qquad U_{\mu 3}^2 = c_\phi^2 s_\psi^2, \qquad U_{\tau 3}^2 = c_\phi^2 c_\psi^2\ . \quad (2)$$

The oscillation probabilities are given by [10]:

$$P(\nu_\alpha \to \nu_\beta) = \begin{cases} 4U_{\alpha 3}^2 U_{\beta 3}^2 S & \text{if } \alpha \neq \beta \\ 1 - 4U_{\alpha 3}^2(1 - U_{\alpha 3}^2)S & \text{if } \alpha = \beta \end{cases}\ , \quad (3)$$

where $S = \sin^2(1.27 m^2 L/E_\nu)$, with m^2, L, and E_ν measured in eV^2, km, and GeV respectively. In this scheme, ν and $\bar\nu$ oscillations in vacuum are indistinguishable.

It has been shown [10] that a useful representation of the parameter space (m^2, ψ, ϕ) is obtained through ($\tan^2\psi$, $\tan^2\phi$) sections at fixed values of m^2. A generic point in the ($\tan^2\psi$, $\tan^2\phi$) plane represents the state ν_3; the lower left and right corners and the upper side represent, asymptotically, ν_τ, ν_μ, and ν_e respectively.

For definiteness, we choose a representative 3ν case:

$$\begin{cases} m^2 &= 2.5 \times 10^{-2}\ \text{eV}^2 \\ \nu_3 &= \sqrt{0.75}\,\nu_\tau + \sqrt{0.20}\,\nu_\mu + \sqrt{0.05}\,\nu_e \end{cases}\ , \quad (4)$$

corresponding to $\psi = 27.3^\circ$ and $\phi = 12.9^\circ$. In Fig. 1, this test case is marked by a black circle ($\bullet$) in the ($\tan^2\psi$, $\tan^2\phi$) plane at $m^2 = 2.5 \times 10^{-2}$ eV^2.

The case in Eq. (4) has the following properties (see also [10]): (1) it is allowed by the available reactor data, as shown in Fig. 1; (2) it is in the sensitivity region of long-baseline experiments; (3) it is outside the sensitivity

region of the running oscillation experiments, CHORUS, NOMAD, KARMEN, and LSND (see [10] and references therein); (4) it is compatible with the indications of an anomalous μ/e flavor ratio in the atmospheric ν flux, and in particular with a value $R_{\mu/e} = (\mu/e)_{\rm data}/(\mu/e)_{\rm theory} \simeq 0.72$, as shown in Fig. 1; and (5) the matrix elements $U_{\alpha 3}$ are hierarchically ordered. We will emphasize the results that remain valid in more general situations.

The adopted value of m^2 is sufficiently high to allow in Eq. (3), for our purposes, the "averaged oscillation" approximation, $\langle S \rangle \simeq 1/2$. In a more refined approach, S has to be computed using the E_ν/L spectrum. Spectral analyses are also necessary to infer the value of m^2. A discussion of such tests is beyond the scope of this work.

Our strategy is the following. For any experiment we define one or more observables, Q_i, that differ from zero in the presence of oscillations. We assume a conservative, plausible estimate of $\pm 20\%$ for the total experimental errors, δQ_i, of the measured signals Q_i. The actual values of the errors are not decisive for our considerations. The δQ_i's will be precisely estimated when the experiments will perform real measurements. In synthesis:

$$\begin{cases} Q_i = 0 \;\rightarrow\; \text{no oscillation} \\ Q_i \neq 0 \;\rightarrow\; \text{oscillation} \;\; (\delta Q_i/Q_i \simeq \pm 20\%) \end{cases} . \qquad (5)$$

We then compute the Q_i's in the representative 3ν test case [Eq. (4)] using the averaged oscillation probabilities, $P_{\alpha\beta} = \langle P(\nu_\alpha \rightarrow \nu_\beta) \rangle$ [Eq. (3)]. Our goal is to study how the starting test values of the mixing angles may be inferred from measurements of the obervables Q_i.

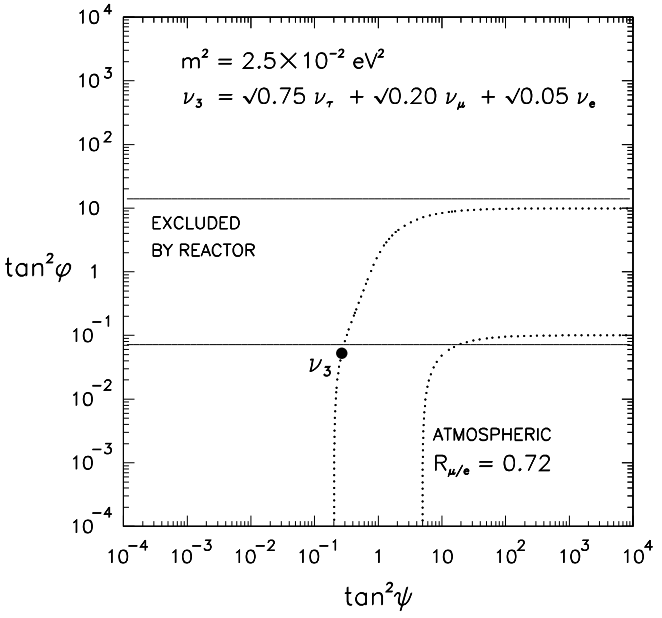

FIG. 1. The representative three-flavor mixing case ($\bullet$) in the ($\tan^2\psi$, $\tan^2\phi$) plane. The horizontal band is excluded by present reactor ν data. The Γ-shaped region is consistent with the indications of the atmospheric neutrino flavor anomaly ($R_{\mu/e} = 0.72$ along the dotted lines). See also Ref. [10].

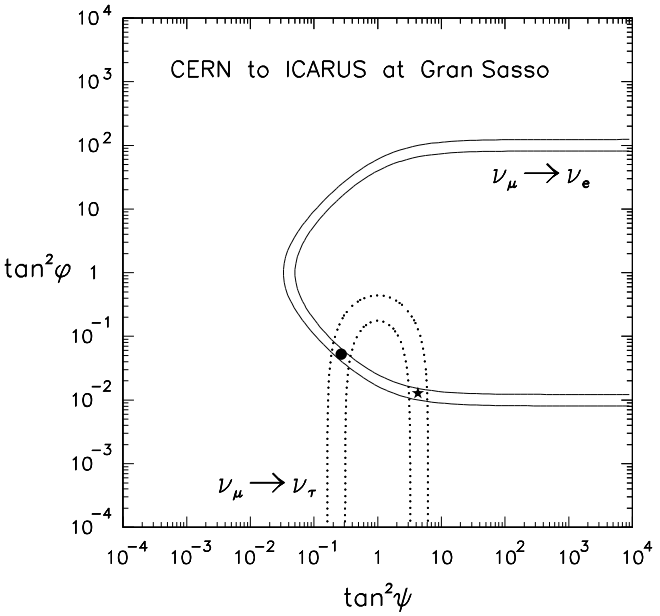

FIG. 2. Allowed bands corresponding to $\nu_\mu \rightarrow \nu_e$ and $\nu_\mu \rightarrow \nu_\tau$ appearance searches at the ICARUS experiment, in the test case ($\bullet$) of Fig. 1. The two bands also intersect at a second point ($\star$), giving rise to a twofold ambiguity in the determination of the mixing angles ψ and ϕ.

III. OSCILLATION TESTS AT ICARUS

The ICARUS detector can identify e-events downstream from a ν_μ beam, thus probing $\nu_\mu \rightarrow \nu_e$ appearance. There are good prospects for direct τ identification. So we also assume that $\nu_\mu \rightarrow \nu_\tau$ appearance searches can be performed with the ICARUS detector.

Two observables can be defined in terms of the number of events $N_{e,\mu,\tau}$ at the detector:

$$Q_{\mu e} \equiv \frac{N_e(\text{observed})}{N_\mu(\text{expected})} = P_{\mu e} \; , \qquad (6)$$

$$Q_{\mu\tau} \equiv \frac{N_\tau(\text{observed})}{N_\mu(\text{expected})} = P_{\mu\tau} \; . \qquad (7)$$

In the 3ν test case [Eq. (4)], the above observables take the values $Q_{\mu e} = 0.02(1 \pm 0.2)$ and $Q_{\mu\tau} = 0.30(1 \pm 0.2)$.

In Fig. 2 we show the corresponding curves of iso-$Q_{\mu e}$ and iso-$Q_{\mu\tau}$. The width of the bands is proportional to δQ_i. The bands intersect at two points. One represents, of course, the "true" test case ($\bullet$). The second point ($\star$) represents a "false" combination of mixing angles. In other words, the determination of (ψ, ϕ) through the values ($Q_{\mu e}$, $Q_{\mu\tau}$) is subject to a twofold ambiguity.

The appearance of a second 3ν solution is not limited to the test case, and cannot be avoided by reducing the errors δQ_i. In fact, the twofold solution arises essentially from the quadratic mixing terms in Eq. (3).

IV. OSCILLATION TESTS AT MINOS

The MINOS detector can identify μ tracks downstream from a ν_μ-beam. It is also expected to identify electrons and thus to be as sensitive to $Q_{\mu e}$ as the ICARUS detector. First we describe two oscillation search methods that use only μ-identification, the T-test and the far/near-test [1]. Then we discuss the e-appearance observable $Q_{\mu e}$.

The T and far/near tests exploit the unoscillated measurements at a second, smaller detector to be placed near the ν-beam source. One separates the events with "one muon track" (1μ) and with "no muon track" (0μ).

At the near detector, the number of events $n_{1\mu}$ and $n_{0\mu}$ are proportional to the ν_μ charged (CC) and neutral current (NC) E_ν-averaged cross sections, $\sigma_{\rm C}$ and $\sigma_{\rm N}$:

$$n_{1\mu} \propto \sigma_{\rm C} \quad , \quad n_{0\mu} \propto \sigma_{\rm N} \quad . \tag{8}$$

At the far detector one also has to include the interactions of ν_e's and ν_τ's. Downstream, 1μ events are produced by: (1) ν_μ CC interactions, and (2) ν_τ CC interactions followed by $\tau \to \mu$ decay. The 0μ events are produced by: (1) ν_μ NC interactions; (2) ν_e CC or NC interactions; (3) ν_τ NC interactions; and (4) ν_τ CC interactions followed by $\tau \to x$ decay, $x \neq \mu$. Thus the number of events $N_{1\mu}$ and $N_{0\mu}$ in the far detector are

$$N_{1\mu} \propto P_{\mu\mu}\,\sigma_{\rm C} + P_{\mu\tau}\,\eta\,\sigma_{\rm C}\,B \ , \tag{9a}$$

$$N_{0\mu} \propto P_{\mu\mu}\,\sigma_{\rm N} + P_{\mu e}(\sigma_{\rm N}+\sigma_{\rm C}) + P_{\mu\tau}[\sigma_{\rm N} + \eta\,\sigma_{\rm C}(1-B)] \ , \tag{9b}$$

where $B = 0.18$ is the branching ratio $(\tau \to \mu)/(\tau \to$ all), and the factor $\eta \simeq 0.31$ [1] accounts for the average reduction of the ν_τ CC cross section due to the τ-mass.

Given Eqs. (8,9), one introduces [1] two ratios, t and T, at the near and far detector respectively:

$$t \equiv \frac{n_{1\mu}}{n_{1\mu}+n_{0\mu}} = \frac{\sigma_{\rm C}}{\sigma_{\rm C}+\sigma_{\rm N}} \ , \tag{10}$$

$$T \equiv \frac{N_{1\mu}}{N_{1\mu}+N_{0\mu}} = \frac{t\,(P_{\mu\mu}+\eta\,B\,P_{\mu\tau})}{1-t\,P_{\mu\tau}(1-\eta)} \ . \tag{11}$$

In deriving the R.H.S. of Eq. (11) we have used the unitarity property $P_{\mu e}+P_{\mu\mu}+P_{\mu\tau}=1$ and the definition of t in Eq. (10). At MINOS energies it is $t \simeq 0.72$ [1].

In the T-test, $T \neq t$ signals neutrino oscillations. A useful observable can be defined as:

$$Q_T \equiv 1 - \frac{T}{t} = 1 - \frac{P_{\mu\mu}+\eta\,B\,P_{\mu\tau}}{1-t\,P_{\mu\tau}(1-\eta)} \ . \tag{12}$$

In the far/near-test, one counts only 1μ events at the two detector distances, $L_{\rm far}$ and $L_{\rm near}$. Neutrino oscillations are signaled by a non-zero value of the quantity:

$$Q_{f/n} \equiv 1 - \frac{N_{1\mu}}{n_{1\mu}}\,\frac{L^2_{\rm far}}{L^2_{\rm near}} = 1 - P_{\mu\mu} - P_{\mu\tau}\,\eta\,B \ . \tag{13}$$

In the 3ν test case, $Q_T = 0.18(1\pm0.2)$ and $Q_{f/n} = 0.30(1\pm0.2)$. The corresponding iso-signal bands are shown in Fig. 3. These Γ-shaped bands largely superpose in the lower part, producing multiple "false" mixing cases ($\circ\cdots\circ$) that have, within errors, the same values of Q_T and $Q_{f/n}$ as the "true" test case ($\bullet$). The multiple solutions (except the highest in ϕ) are allowed by present reactor data, and are consistent with the atmospheric ν anomaly (cf. Figs. 1 and 3). The larger the errors (δQ_i), the more ambiguous is the 3ν interpretation of the combined Q_T and $Q_{f/n}$ signals.

The T and far/near tests are not very effective in discriminating among 3ν cases, since a large fraction of their signal is induced by a disappearance probability, $P_{\mu\mu}$ [Eqs. (12,13)]. If limited to Q_T and $Q_{f/n}$, the 3ν-mixing searches at MINOS may not be much more constraining than a pure μ-disappearance experiment as BNL E889 [4] (that, incidentally, is not proceeding [2]).

Therefore it is very important that the MINOS detector probes e-appearance directly. As shown in Fig. 3, the addition of the $Q_{\mu e}$-test [Eq. (6)] reduces the multiple solutions ($\circ\cdots\circ$) to the same two cases ($\bullet$ and $\star$) as in ICARUS (Fig. 2). The comparison of Figs. 2 and 3 shows that, unfortunately, the ambiguity is not solved by combining the MINOS and ICARUS tests.

If direct τ-identification were possible at MINOS ($\nu_\mu \to \nu_\tau$ appearance), the oscillation searches would be corroborated, since the two solutions ($\bullet$ and $\star$) would sit at the intersection of 4 bands in the ($\tan^2\psi$, $\tan^2\phi$) plane—an overconstrained situation. However, the 3ν-mixing ambiguity would still remain unsolved.

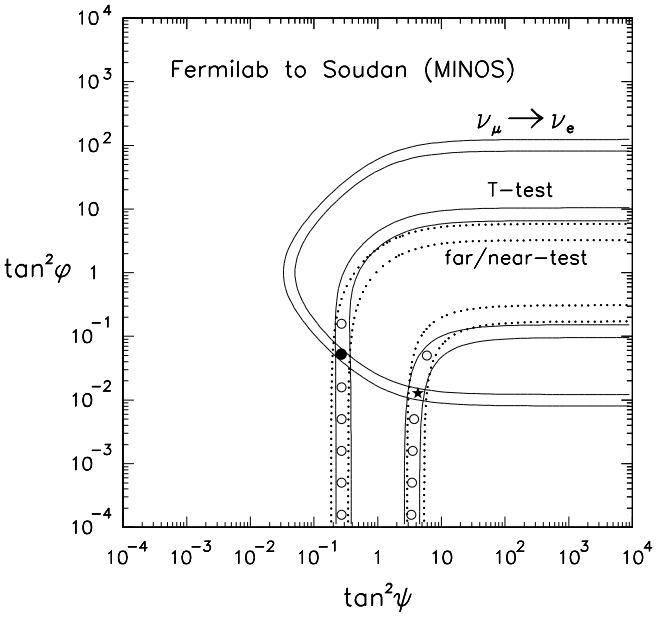

FIG. 3. Allowed bands corresponding to three oscillation tests at the MINOS experiments: T-test, far/near-test, and $\nu_\mu \to \nu_e$ appearance search. The combination of the T and far/near tests allows multiple solutions ($\circ\cdots\circ$). Adding the $\nu_\mu \to \nu_e$ test, only two solutions remain ($\bullet$ and $\star$) as in Fig. 2.

The addition of atmospheric ν data in the usual format of μ/e flavor ratio is not particularly helpful, being very similar to the T-test (cf. Figs. 1 and 3). Flavor-separated data [12] could be more effective in 3ν mixing cases.

The two possible $\nu_\mu \to \nu_\mu$ and $\nu_\mu \to \nu_e$ oscillation tests at the planned SuperKamiokande experiment [3] are similar to the MINOS tests. However, the uncertainties [3] are expected to be larger, and the 3ν-mixing discrimination power should be poorer.

As in MINOS, the RICH [6] and NOE [7] detectors can distinguish 1μ and 0μ events and perform a $1\mu/(1\mu+0\mu)$ test. In absence of a near-detector at CERN, the normalization of their ν-rates has to rely upon simulations.

V. OSCILLATION TEST AT REACTORS

In reactor experiments, a single neutrino oscillation search is performed, namely the ν_e-disappearance test:

$$Q_{ee} \equiv 1 - P_{ee} \ . \tag{14}$$

In the 3ν-mixing test case [Eq. (4)], $Q_{ee} = 0.095(1 \pm 0.2)$. This value is in the sensitivity region of the Chooz [8] and San Onofre [9] experiments.

In Fig. 4 we show the corresponding iso-signal stripes. It can be seen how the supplementary reactor ν information singles out the "true" mixing case ($\bullet$) and solves the ICARUS and MINOS ambiguity.

However, at slightly smaller test values of ϕ the reactor experiments become rapidly less sensitive and might not be able to select the "true" solution within the errors.

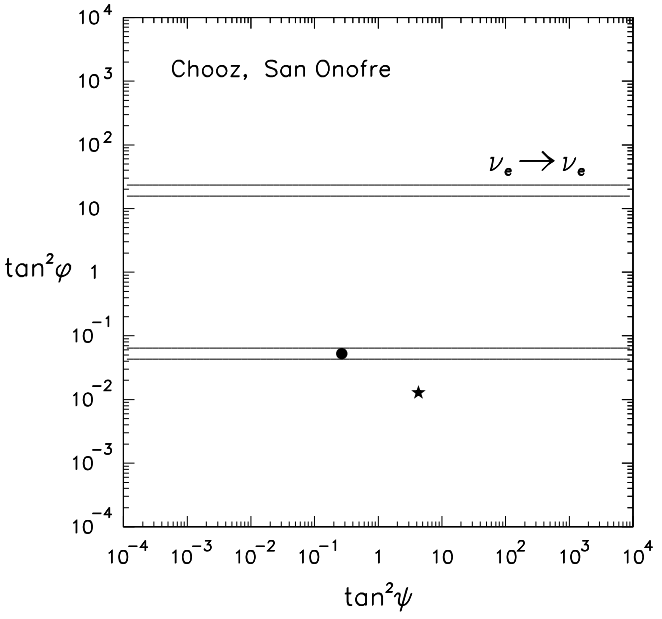

FIG. 4. Allowed bands corresponding to the $\nu_e \to \nu_e$ disappearance test at reactors (Chooz, San Onofre). This test appears to solve the twofold ambiguity between the "true" ($\bullet$) and "false" ($\star$) 3ν mixing solution in Figs. 2 and 3.

VI. SUMMARY

We have studied tests of three-flavor mixing in future long-baseline ν oscillation experiments. We have adopted a specific, simple 3ν-mixing case [Eq. (4)], highlighting the aspects that have a more general validity.

We have considered five observables, $Q_{\mu e}$, $Q_{\mu\tau}$, Q_T, $Q_{f/n}$, and Q_{ee}, that assume non-zero values in the presence of oscillations. A large fraction of the Q_T and $Q_{f/n}$ oscillation signals (MINOS) is related to μ-disappearance, and their combination may not be very effective in constraining 3ν-mixing cases. The flavor-appearance observables $Q_{\mu\tau}$ (ICARUS) and $Q_{\mu e}$ (ICARUS, MINOS) allow a better resolution of 3ν mixing angles, modulo a residual twofold ambiguity. The addition of the reactor observable Q_{ee} (Chooz, San Onofre) may solve the ambiguity and select a unique 3ν signal.

We thank J. H. Cobb, M. Goodman, P. I. Krastev, and D. Petyt for reading the manuscript and for useful information and suggestions. We thank the organizers of the Gran Sasso Long-baseline Workshop (Gran Sasso, Italy, 1995), where preliminary results of this work were presented. This work was supported by INFN and by the Institute for Advanced Study.

[1] MINOS Collaboration proposal, Fermilab Reports No. NuMI-L-63 and No. NuMI-L-79 (unpublished).
[2] Subpanel of the High Energy Physics Advisory Panel on Accelerator-based Neutrino Oscillation Experiments, U.S. Department of Energy Report No. DOE-ER-0662, 1995 (unpublished).
[3] KEK-PS and SuperKamiokande Collaboration proposal, University of Tokyo report, 1995 (unpublished).
[4] E889 Collaboration proposal, Brookhaven National Laboratory Report No. BNL-52459 (unpublished).
[5] ICARUS Collaboration proposal, Laboratori Nazionali del Gran Sasso (LNGS, Italy) Reports No. LNGS-94-99 (Vol. I and II) and No. LNGS-95-10 (unpublished).
[6] T. Ypsilantis *et al.*, CERN Report No. CERN-LAA-96-02 (unpublished).
[7] NOE Collaboration, Letter of intent to the Scientific Committee of Gran Sasso Laboratory (Dec. 1995), University of Naples Report (unpublished).
[8] Chooz Collaboration proposal, Collège de France report, 1993 (unpublished).
[9] San Onofre Collaboration proposal, California Institute of Technology report, 1994 (unpublished).
[10] G. L. Fogli, E. Lisi, and G. Scioscia, Phys. Rev. D **52**, 5334 (1995).
[11] G. L. Fogli, E. Lisi, and D. Montanino, Phys. Rev. D **49**, 3626 (1994); Astropart. Phys. **4**, 177 (1995).
[12] G. L. Fogli and E. Lisi, Phys. Rev. D **52**, 2775 (1995).